Jurnal Kejuruteraan 34(6) 2022: 1149-1168
https://doi.org/10.17576/jkukm-2022-34(6)-15

Cyber-Attack and Reliability Monitoring of The Synchrophasor Smart Grid Network

Atul Kumar Yadav & Vasundhara Mahajan*

Electrical Engineering Department, Faculty of Engineering, Sardar Vallabhbhai National Institute of Technology, Surat, Gujarat, India, 395007

**Corresponding author: vasu.daygood@gmail.com*

Received 7 March 2022, Received in revised form 7 April 2022
Accepted 5 May 2022, Available online 30 November 2022

ABSTRACT

The recent advancement of synchrophasor measurements technology in the conventional power grid can monitor and control the state variables of the network very accurately at a high sampling rate in real-time. The complete observability of system states can be achieved through the Phasor Measurement Unit (PMU). The inclusion of a zero injection bus (ZIB) optimized the total number of PMU requirements for complete observation of the synchrophasor network. The communication channels between measurement devices and control centers are highly vulnerable to cyber threats. Thus, an anomaly that occurs with PMU devices during a cyber-attack can affect the system's reliability. Therefore, monitoring the reliability of the synchrophasor network has become essential for healthy power operation. Synchrophasor measurement technology can enhance wide-area surveillance and security functionality. However, the dependability of such technologies in the context of information network accessibility has yet to be investigated in a coherent model. Growing electric grid defence levels to mitigate the impact of cyber-attacks is essential. The cumulative effect of synchrophasor network observability and reliability is discussed in this paper by optimizing the number of PMUs deployed and the interruption load that occurs during an anomaly with PMU while taking ZIB into account.The backup PMU deployment modeling is also presented to secure the reliability and observability of the grid network during an anomaly occurs with PMU. The indices, Interrupted Load Probability Index (ILPI) and Expected Demand Not Supplied (EDNS), are used to evaluate the reliability of synchrophasor grid networks by integrating the state probability of PMU unavailability due to cyber intrusion.

Keywords: ZIB; optimal PMU deployment; synchrophasor grid observability; reliability indices; cyber intrusion

INTRODUCTION

AIM AND MOTIVATION

Synchrophasor measurements technology is making the conventional grid smarter to observe the states of the network in real-time. The measurements devices such as PMU and Phasor Data Concentrator (PDC) are highly vulnerable to abnormalities that occur due to cyber intrusion. Therefore, cyber-attack on PMU devices or communication links between the control center needs to monitor for maintaining the reliability and observability of the network. The reliability of the synchrophasor network can be enhanced by securing the availability of measurements devices (Patil and Thosar 2017; Vaiman, Quint et al. 2018). The network consists of the ZIB is advantageous for the observation of states of the network. If one incoming and one outgoing transmission line is connected at a ZIB then the current in both the line will be the same by applying the Kirchhoff's Current Law (KCL) at ZIB. On the other hand, if the bus is not a ZIB then the incoming current will not be equal to the outgoing current. Therefore, observability of states of such paths can be obtained by placing the extra PMU in the system (Deng, Bian et al. 2019). The concluding remarks resulting that the number of PMU requirements for complete states observation of the network will be more, if the effect of ZIB is excluded. Thus, the modelling of optimal placement of PMU devices in the network obtains with the inclusion of ZIBs. The motivation for modelling the objective function is based on the optimization of the number of PMUs required for the complete observation along with the integration of optimization of interrupted load for improving the reliability of the network during cyber-attack (Popov, Mokeev et al. 2020; Mustafa, Wang et al. 2021).

BACKGROUNDS

Nowadays, wide-area monitoring of power system networks is becoming easier due to advancements in synchrophasor technology. A PMU deployed on a particular bus can directly measure the voltage phasor of the bus and also the current phasor of all the transmission lines connected to this bus at a very high sampling rate in real-time. Therefore, indirectly, the voltage phasor of all the buses connected to this particular PMU bus can be obtained using nodal analysis (Kovalenko, Mukhin et al. 2020). The system buses neither connected to the generator nor load is known as ZIB. The inclusion of ZIB also ensures network observability by reducing the optimal number of PMUs in the grid network. Thus, it is not required to place the PMU on each bus for complete observability of the synchrophasor network. By doing so, the number of PMU deployments in the network can be reduced by optimization techniques for the complete observability of the network. Several studies on the optimal deployment of PMU are discussed with the consideration of different objectives such as PMU installation cost, voltage stability, and many more (Blair, Burt et al. 2018).

TABLE 1. An assortment of various research area contribution in synchrophasor power grid

Research area	Contributions to research study	References
PMU placement modelling/ Network observability	• A integer linear programing (ILP) based algorithm obtaining the optimal allocation of PMU devices by considering the effect of ZIB, a test case performed on IEEE-14, 30, 39, and 118 bus system with objective to find the optimal number of PMU for observability.	(Abdulrahman & Radman 2018)
	• Binary particle swarm optimization based algorithm minimizing the installation cost of PMU, a test case on 14, 30, 57, and 246-bus system.	(Babu & Bhattacharyya 2016)
	• Two mathematical programing algorithm discussing the optimization of number of PMU in the test system, one method is mixed integer linear programing (MILP) and other is non-linear programming (NLP).	(Almunif & Fan 2020)
	• The paper integrate the optimal placement of PMU devices, and vulnerability. Prior identifying critical buses to enhance the aspect of fault tolerance.	(Almasabi & Mitra 2019)
Cyber-attack in smart grid	• Characterization and optimization based observability of network obtain during cyber-attack on PMU devices using the greedy algorithm for optimal PMU placement.	(Ding, Xu et al. 2021)
	• The paper presenting the network obsrvability in post attack scenarios by optimizing the restoration of PMU devices, mixed integer linear programming algorithm obtaining the observability after recovering from massive attacks.	(Edib, Lin et al. 2020)
	• The cyber intrusion detection and localization of cyber-attack on PMU based synchrophasor network followed by correction in the measurements data during the attack	(sadat Khalafi, Dehghani et al. 2021)
	• A robust technique elaborates for detection of cyber-attack, injecting false data to dynamic state estimator that delivered the measurements data to PMUs.	(Chakhchoukh, Lei et al. 2019)
Reliability analysis	• The optimal allocation of PMU devices in distribution network is modelled for reliability of state estimation.	(Gholami, Abbaspour et al. 2020)
	• Reliable zero injection (ZI) observation is presented, reliability of ZI observation improved through depth of ZI observation.	(Lu, Wang et al. 2018)
	• Component reliability incorporation for incremental PMU deployment model using the analytical hierarchical based technique, the observability is tested for 90 bus real power network of eastern India.	(Kumar, Tyagi et al. 2018)
	• Reliability based approach to locate the micro PMU in the distribution network for observability during contingencies scenarios.	(Abdolahi, Taghizadegan et al. 2021)

The PMU devices measuring data can be modified by the cyber intrusion. Therefore, to prevent the stamped data of PMU, an alternative should be deployed in the network to maintain the observability and reliability of the grid system. Previously, conventional system reliability was primarily determined by load interruption, load demand, transmission line switching, generating unit outages, and bus-bar and circuit breaker failure.The recent development of synchrophasor technology has emerged with new reliability challenges for future study. These challenges are monitoring and controlling the communication channels, preventing PMUs from cyber threats, and the failure rate of measuring devices, etc (Peng, Nair et al. 2013, Nageswara Rao, Vijaya Priya et al. 2019). A typical synchrophasor grid network for a nine-bus system subjected to cyber threats at communication channels followed by super PDC and control room is shown in Figure 1. The contribution of several research area of the particular field is assorted in Table 1. Load forecasting is major part of system reliability assessment (Fadhilah, Mahendran et al. 2009).

Information and communication technology (ICT) is an essential component of the synchrophasor network. It improves transmission network monitoring and prevention, supply reliability, confidentiality, and self-healing capabilities by utilising intelligent architecture. Innovations like active utility grids, intelligent buildings and organizations, variable network grading, specific safety systems, and market planning activities are used to incorporate ICT infrastructures into the electricity system. The implementation of such innovations seems to have a positive impact on synchrophasor network reliability and observability. Unfortunately, due to Internet of Things (IoT) regulations, such infrastructures are inherently vulnerable to failures and information security risks, which might affect smart grid reliability. As a result, this study evaluates research that goes beyond conventional reliability analysis and includes the influence of ICT interfaces on system-wide dependability as well as the implications of cyber infrastructure breakdowns. Furthermore, the report provides quantitative and qualitative data on the influence of ICT integrated with a range of innovative advancements on current electricity grid reliability (Jimada-Ojuolape and Teh 2020).

ICT systems are becoming an indispensable part of everyday activities, and their incorporation into the synchrophasor network is critical. ICTs enable the efficient integration of all electric grid participants' actions, resulting in a much more expensive and ecological electrical network. Sophisticated management and review, bidirectional interaction among consumers and electrical infrastructure components, providing security and safety, and consciousness properties will all be features of the electrical synchrophasor network. Furthermore, despite the numerous benefits of ICTs, their deployment in the transmission system has certain downsides, including component breakdowns, interdependency inadequacies, and information security vulnerabilities. These flaws may have a negative influence on the electricity grid's reliability (Jimada-Ojuolape and Teh 2020).

Distinct information network components known as network nodes are associated through a medium of interaction to exchange information in a cyber-physical system. An information network infrastructure is a framework used to interconnect different nodes inside a cyber-physical system, and it governs how data is communicated among the nodes. There are several configuration types used, including bus, line, ring, point-to-point, star, and mesh configurations.

In line configuration, one node is connected to another in a series, forming a line. Under this configuration, data is communicated by transferring it from the starting point to another node until it arrives at its final location. This configuration is comparatively simple to implement. However, information cannot arrive at its final location if a node fails. A coordinator node serves as a catalyst in a star configuration, and it is linked to two or even more receiver nodes. Except through the coordinator node, the linked receiver nodes are unable to interact directly. A node in a ring configuration connects to two neighboring nodes in a fashion to make a loop sequence. In a mesh configuration, every node can interact and share information with each other. Approaches for surveilling PMU's relevant information are described to identify inaccurate information. But its consequences on grid reliability are not accurately measured. (Jimada-Ojuolape and Teh 2021).

Research gap and objective modelling: There are several research articles on the topic of optimal PMU placement (OPP), reliability studies are limited to distribution networks, and cyber threats present attack and detection techniques during the attack. This paper integrates the reliability analysis of generation and transmission systems with modified reliability indices subjected to the state probability of optimally deployed PMUs. The load interruption is caused due to a cyber-attack on PMUs, affecting the reliability of the synchrophasor network. Therefore, backup PMU installation modelling preserves the reliability and observability of the synchrophasor network.

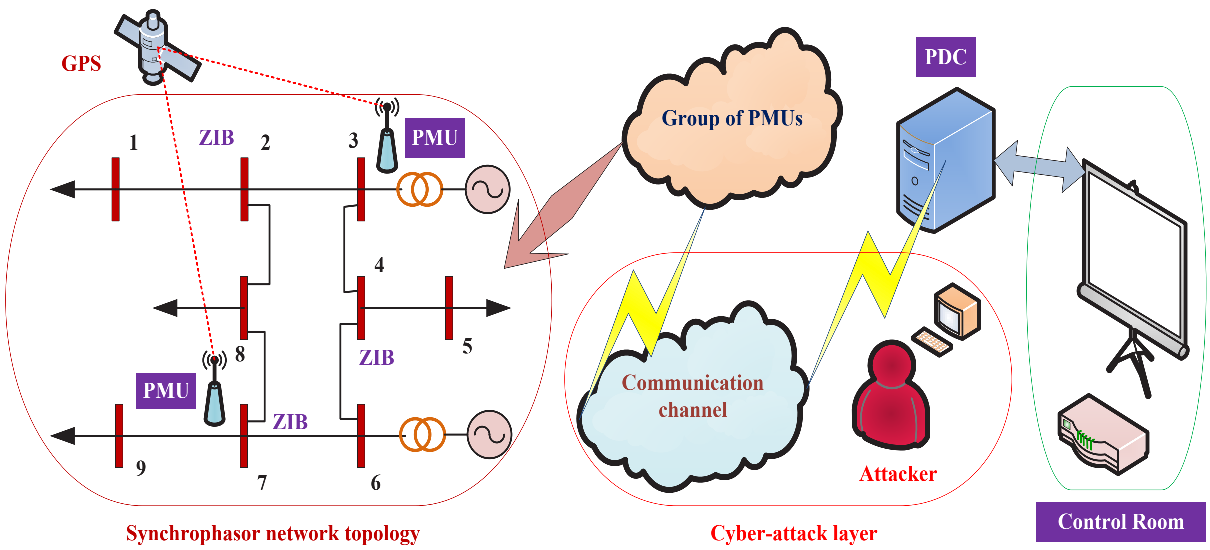

FIGURE 1. A typical synchrophasor smart grid network topology

CONTRIBUTION

The paper shows the cumulative effect of observability and reliability for synchrophasor smart grid networks with the inclusion and exclusion of ZIB in the system. Observability can be obtained by placing the optimal number of PMUs in the network for complete state analysis, and reliability can be achieved by optimizing the interrupted load caused by several contingencies such as transmission line switching, an anomaly with PMU due to cyber-attack (Yadav and Mahajan 2021). The Reliability Test System (RTS-79) IEEE 24-bus is used as a synchrophasor network by deploying the optimal PMU across the buses of conventional networks for the analysis of the objective of the paper. Therefore, the main contributing part is discussed in two subsections.

1. Synchrophasor network observability: A conventional grid with synchrophasor technology is rapidly integrating into the modern era.The state's analysis of the network variables can be observed in real-time by introducing the synchrophasor measurement devices. The observability of the network can be ensured by taking the optimizing function as binary digit variables for PMU deployment. The function of the PMU is such that it will observe all buses connected to a PMU bus. The inclusion of the effect of ZIB in the network can minimize the total number of PMU requirements for complete state observation of the grid network. Therefore, the objective function is modelled based on the inclusion or exclusion of ZIB in the system, following the observability constraints. The system observability is also studied for the line contingency and anomalies arise with PMU devices during the cyber intrusion. The backup PMU deployment model is formulated for anomaly behaviour of the PMU to ensure the complete observability of the synchrophasor grid network. By doing so, grid observability can be enhanced during a cyber-attack on PMU-allocated buses.
2. Synchrophasor network reliability: The conventional power system reliability is assessed by observing load curtailments, generating unit availability and unavailability; transmission line switching rate; load demand; generating capacity; and so on.The conventional power system network is becoming a synchrophasor network with the installation of PMU devices across the system buses. By doing so, the system becomes more vulnerable to cyber intrusion. Therefore, monitoring the measurement devices and communication links between them becomes essential to maintain the reliability and observability of the network. The synchrophasor smart grid system reliability can be evaluated by integrating the availability and unavailability of PMUs devices or communication channels into the conventional system components' availability. Therefore, the reliability indices used for the analysis of the reliability of the synchrophasor network become updated by integrating the state probability of PMU availability or unavailability during anomaly events with PMU devices. The parameters used for the reliability test of the synchrophasor grid are defined by the Interrupted Load Probability Index (ILPI) and Expected Demand Not Supplied (EDNS).

The paper is organised into several sections and subsections: Section 2 represents the objective function modelling for complete observability and reliability of the grid network. Section 3 provides a brief idea about the test system for observing the paper's objective. Section 4 covers the simulation results and discussion for complete observability and reliability of the network during an anomaly with PMU devices caused by a cyber-attack, section 5 summarised the concluding remarks of the whole paper, followed by research references.

METHODOLOGY

The smart grid system observability can be improved by optimal allocation of synchrophasor measurements devices, i.e., PMU. There are several research articles introducing the optimal placement of PMU in the grid network. The advancement of synchrophasor technology in the grid network makes the system more vulnerable to cyber threats. Therefore, ensuring system reliability has become a focus area in the field of synchrophasor networks (Noureen, Roy et al. 2017, Sushma and Jyothsna 2018). This paper includes the complete observability of the network along with the consideration of the effect of interruption load caused due to several contingencies, such as transmission line switching, an anomaly with PMU due to cyber-attack, The cumulative objective of this paper includes the minimization of interrupted load caused by several contingencies along with the minimization of the cost of PMU that has to be placed in the network for complete observability. Equation (1) shows the objective function used for complete observation of the network followed by an improvement in the reliability of the system. The observability and reliability of the synchrophasor network are studied through the inclusion of ZIB in the system. The observability constraints for optimal deployment of PMUs in the network with consideration of the effect of ZIB are shown in equation (2-4). The load flow constraints for minimization of interrupted load are subjected to the following equality and inequality constraints as shown in the equations (7–15). The objective function is optimized through the Particle Swarm Optimization (PSO) technique by considering the listed boundary constraints for observability and reliability.

$$Min \quad \sum_{b=1}^{Nb} CV_b^{md} * x_b + \sum_{b=1}^{Nb} LC_b * CV_b^{li} \tag{1}$$

Observability constraint: subjected to-

$$O_b \geq 1 \quad \forall b \in B \tag{2}$$

$$O_b = \sum_{i=1}^{Nb} f_{bi} * x_i + \sum_{i=1}^{Nb} f_{bi} * y_{bi} \quad \forall b \in B \tag{3}$$

$$\sum_{b=1}^{Nb} y_{bi} = \begin{cases} 1, & If \ bus \ i \ is \ ZIB \\ 0, & otherwise \end{cases} \tag{4}$$

Where,

$$x_b = \begin{cases} 1, & If \ a \ PMU \ is \ deployed \ at \ bus \, b \\ 0, & otherwise \end{cases}$$

$$f_{bi} = \begin{cases} 1, & If \ b = i \\ 1, & If \ b \ and \ i \ are \ connected \\ 0, & otherwise \end{cases} \tag{5}$$

Load flow constraints observing interrupted load: subjected to-

$$\theta_b^{\min} \leq \theta_b \leq \theta_b^{\max} \quad \forall b \in B \tag{7}$$

$$AP_{gu}^{\min} \leq AP_{gu} \leq AP_{gu}^{\max} \quad \forall gu \in GU \tag{8}$$

$$-LF_{tl}^{\min} * \Omega_{tl} \leq LF_{tl} \leq LF_{tl}^{\max} * \Omega_{tl} \quad \forall tl \in TL \tag{9}$$

$$0 \leq LC_b \leq LD_b \quad \forall b \in B \tag{10}$$

$$\sum_{b \in B} CN_{b,gu} * AP_{gu} - \sum_{tl \in TL} IN_{b,tl} * LF_{tl} = LD_b - LC_b \tag{11}$$

$$\sum_{b \in B} IN_{b,tl} * B_{tl} * \theta_b - LF_{tl} + (1 - \Omega_{tl}) * M \geq 0 \tag{12}$$

$$\sum_{b \in B} IN_{b,tl} * B_{tl} * \theta_b - LF_{tl} - (1 - \Omega_{tl}) * M \leq 0 \tag{13}$$

$$\sum_{tl \in TL} (1 - \Omega_{tl}) \leq J^{\max} \tag{14}$$

$$\Omega_{tl} \in \{0,1\} \quad tl \in TL \tag{15}$$

DIRECT AND INDIRECT OBSERVABILITY ANALYSIS OF BUSES THROUGH PMU WITH CONSIDERATION OF ZIB

A PMU deployed on a bus can correctly measure the bus phasor voltage and current phasor of each transmission line connected to it in real-time. A synchrophasor smart grid network is preserved as a complete observable if all the states (bus voltage magnitude and angle phasor) are well known, directly or indirectly, at each bus. The observability of the power grid network is categorised into two parts: numerical and topological observability. Numerical observability can be analyzed through state estimation, but due to the large computational burden, it is not a preferable approach to examine the optimum solution for the PMU deployment. The grid network is said to be topologically observable if there is a spanning tree of full rank in the grid network. The following steps can be pointed out to make the network topologically observable.

1. If a PMU is deployed on any particular bus, then it has direct observable characteristics from the PMU. The other buses connected to the PMU bus can be considered indirectly observable. The PMU will measure the phasor voltage of the particular bus and the current phasor of all the transmission lines connected to this bus. From Figure 2(a), bus-1 is directly observable by placing the PMU at this particular location, and the rest of the connected buses 2, 3, and 4 can be indirectly observable.
2. For a transmission line is connected between two buses, and if the voltage phasor and current phasor of one end of the transmission line are known, then by using Ohm's law the voltage phasor at the other end of the transmission line can be obtained. This can make the system bus indirectly observable.
3. Similarly, if the voltage phasor of both ends of a transmission line is known, then the current phasor of the line can be obtained by using Ohm's law. In this case, the line current becomes indirectly observable.
4. For an unobservable ZIB, if the voltage phasor of all the buses connected to it is known, the voltage phasor of ZIB can be calculated by applying the KCL at ZIB. From Figure 2(b), bus 2, 3, and 4 are indirectly observable, which means the voltage phasor of all these buses is well known to us. As bus-1 is ZIB and unobservable, the voltage phasor of this bus can be obtained by applying KCL at the node of ZIB. By doing so, bus-1 becomes indirectly observable.
5. For a directly or indirectly observable ZIB, if the voltage phasor of all the other connected buses is known except one, then the voltage phasor of the unknown bus can be calculated by using KCL at the ZIB. From Figure 2(c), Bus 1, 2, and 4 are indirectly observable, which means the voltage phasor at all these buses is known to us. As bus-1 is ZIB, by applying KCL to this bus, the voltage phasor at bus 3 can be obtained. By doing so, the initially unobservable bus-3 becomes indirectly observable.
6. From Figure 2(d), the PMU is placed on bus-1, so the phasor voltage of buses-1 and -2, as well as the current phasor of lines 1-2, can be obtained by the PMU in real-time. As bus-2 is not a ZIB, therefore, the current phasor of lines 1-2 and 2-3 will not be the same. Thus, the voltage phasor of the bus-3 cannot be calculated. This results in only bus-1 and bus-2 being observable. Now, by considering bus-2 as ZIB in Figure 2(d), the current phasor of transmission line 1-2 and line 2-3 will be the same. Thus, the voltage phasor of bus-3 can be obtained and it will become observable. Therefore, the concluding remarks of the observation are that the inclusion of ZIB in the system can reduce the number of PMU deployments in the grid network for complete observability. Figure 2(e-f) represents the influence of ZIB consideration in the network. By making bus-2 as ZIB, the current phasor of line 2-3 $I_{calculated}$ and voltage phasor of bus-2 $V_{2(calculated)}$ can be easily obtained.

The acquired array of estimation problems can be used to perform quantitative observability. The framework is said to be completely eobservable if the acquired array has a full column rank. Despite a few benefits, the quantitative approach's main drawback is its large processing challenge. Furthermore, a large number of degrees of freedom in the measurement array may result in an incorrect solution. A structural graph represents the electric grid in a topological observability assessment. The graph has "N" vertices indicating the power grid bus location and "E" edges indicating the grid branches linking with the buses. The topological approach seeks the optimal PMU deployment such that every bus in the system can be observed by at least one PMU. Simple topological quantitative measurements approach solely based on PMU measured data is presented.

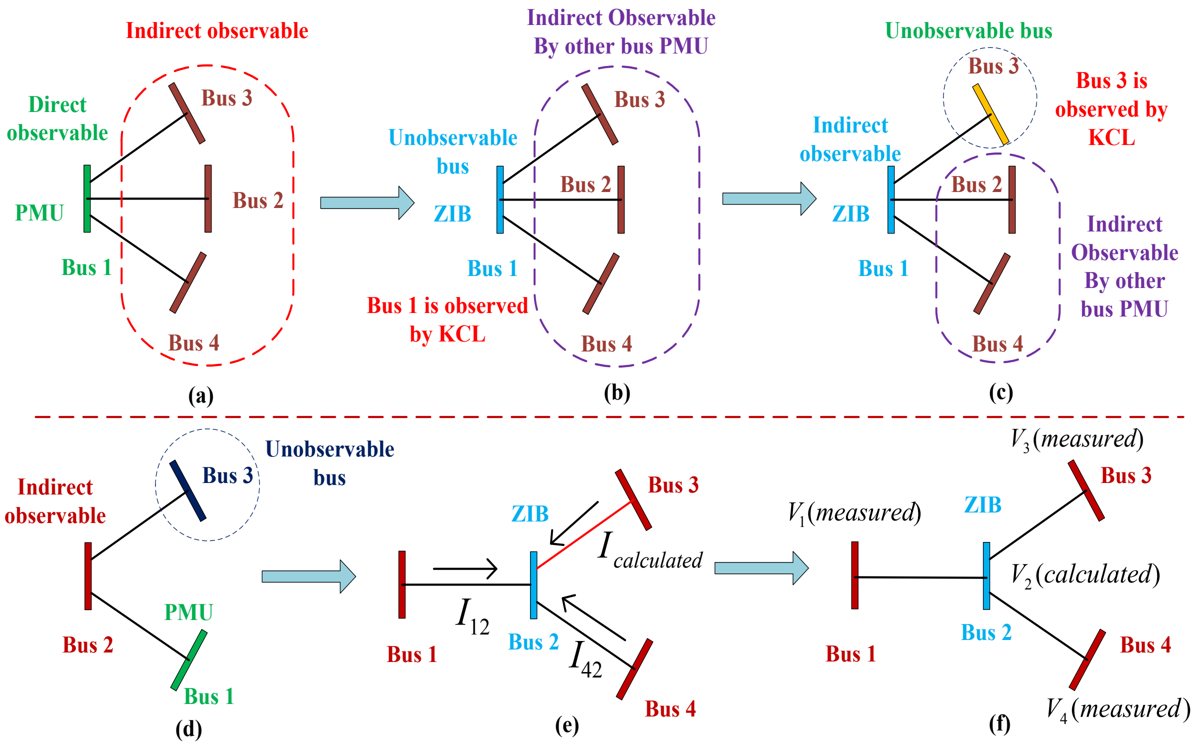

FIGURE 2. Synchrophasor network topological observability due to optimal PMU deployment in the system with and without considering the effect of ZIB

MODELLING OF ZIBS IN OBSERVABILITY CONSTRAINTS

When there is no generating source or load demand mentioned for the specific bus, the power system bus is preferred as ZIB, i.e., the net power injection must be zero at the corresponding bus. By doing so, the total number of PMU deployments can be optimized in the synchrophasor smart grid network. The consideration of the ZIB effect results in an extra measurement equation followed by an auxiliary binary variable assigned to the particular individual ZIBs. System observability can be ensured with the following contribution from ZIB: if all the buses connected to ZIB are observable except one (maybe ZIB or other connected buses), then the observability can be obtained for the unobservable bus by applying the KCL at ZIB. A new auxiliary binary variable y_{bi} is allocate to all the buses connected to ZIB and ZIB itself also. The values of y_{bi} is equal to one represents that bus b receives one computational contribution from ZIB bus i. The constraints in such situation become modified with equation. The synchrophasor network topology of nine-bus system as shown in Figure 1 is used to illustrate the following equation to find the optimal number of PMUs in the system for complete observation of the grid. In this 9-bus system, there are three ZIBs numbered as buses, 2, 4 and 7. The observability constraints of such a system are signified as shown in equations.

$$O_1 = x_1 + x_2 + y_{12} \geq 1 \tag{16}$$

$$O_2 = x_1 + x_2 + x_3 + x_8 + y_{22} \geq 1 \tag{17}$$

$$O_3 = x_2 + x_3 + x_4 + y_{32} + y_{34} \geq 1 \tag{18}$$

$$O_4 = x_3 + x_4 + x_5 + x_6 + y_{44} \geq 1 \tag{19}$$

$$O_5 = x_4 + x_5 + y_{54} \geq 1 \tag{20}$$

$$O_6 = x_4 + x_6 + x_7 + y_{64} + y_{67} \geq 1 \tag{21}$$

$$O_7 = x_6 + x_7 + x_8 + x_9 + y_{77} \geq 1 \tag{22}$$

$$O_8 = x_2 + x_7 + x_8 + y_{82} + y_{87} \geq 1 \tag{23}$$

$$O_9 = x_7 + x_9 + y_{97} \geq 1 \tag{24}$$

$$y_{12} + y_{22} + y_{32} + y_{82} = 0 \tag{25}$$

$$y_{34} + y_{44} + y_{54} + y_{64} = 0 \quad (26)$$

$$y_{67} + y_{77} + y_{87} + y_{97} = 0 \quad (27)$$

Optimizing the number of PMUs deployment in the system following through equations, as constraints yields:

$x_3 = 1$, $x_7 = 1$, $y_{21} = 1$ and $y_{45} = 1$ the list of all other variables are zero. The results clarify that the deployment of PMU at two buses i.e. bus-3 and bus-7 can make the system complete observable. The unobservable bus-1 can be made observable by applying KCL at zero injection bus-2, similarly, the unobservable bus-5 can be made observable by applying KCL at zero injection bus-4, the rest of other buses 2, 3, 4, 6, 7, 8, and 9 are directly or indirectly observable by the PMU placed at bus-3 and bus-7.

RELIABILITY ANALYSIS BY CONSIDERING ANOMALY WITH PMU DUE TO CYBER-ATTACK

As the use of synchrophasor technology grows in recent grid observations, the reliability of such a system must be a primary concern in the current era.The deployment of communication-based devices such as PMUs and PDCs is highly focused on preventing cyber threats from interfering with communication channels.Therefore, backup PMU placement is an alternative to observing the complete system during anomalies with these devices. Therefore, by doing so, the system's reliability and observability can be monitored in real-time scenarios (Vaiman, Energy et al. 2018, Jimada-Ojuolape 2021). The Interrupted Load Probability Index (ILPI) of the system during an anomaly with PMU can be represented as the multiplication of load loss probability during the healthy condition of PMU and loss of PMU probability. The other reliability index Expected Demand Not Supplied (EDNS) during cyber-attack scenarios can be mathematically modelled as the multiplication of expected demand not supplied during the normal condition of PMU and the expected PMU requirement not available. These two indices are evaluated for the reliability analysis of the synchrophasor smart network. Equation (28–29) shows the mathematical formulation of these two reliability parameters.

$$ILPI_S^{AP} = \left(\sum_{LC \neq 0} LOLP_S^H \right) * \left(\sum_{EPR \neq 0} \Pr_{st} \right) \quad (28)$$

$$EDNS_S^{AP} = \left(\sum_{\substack{b \in B \\ c \in C}} LC_b * \Pr_i * SR_{tl} \right) * \left(\sum_{p \in P} \Pr_{st} * EI \right) \quad (29)$$

PARTICLE SWARM OPTIMIZATION (PSO)

Placing PMUs first on the bus with the most incident branches is often not the best PMU deployment solution. Because many buses with single or multiple incident branches are isolated from observation if a large number of incident branches are monitored first with PMU buses, many buses with single or multiple incident branches are isolated from observation if not all of these buses are ZIBs. PMU must set aside time specifically for the observation of all these isolated branches. This observation suggests a method for varying the randomness of PMU placement across system buses. As a result, the PSO algorithm is used for network observation with a random selection of buses to deploy the PMU in order to achieve the global best position (optimal solution). In each iterative process of the PSO optimization technique, a cluster of selected particles will search for the global best solution. Each particle is given a position and a velocity in order to acquire the current local best solution while moving towards the global best centre point (Rahman, Zobaa et al. 2015). Figure 3 shows the flow chart to obtain the objective of the paper using the PSO algorithm. This consists of three-layer observations to be integrated into the constraints to obtain the optimal solution for PMU deployment using PSO. The proposed approach will take information from connectivity matrix entries for observability assessment and then load flow data to evaluate the interruption load for reliability testing. The optimal fitness function value results in the optimal allocation of PMU buses as well as the optimal load interruption during the load flow analysis. Equation (30-31) represents the mathematical procedure of reaching at global best to find the optimal solution.

$$Y_m^{i+1} = Y_m^i + V_m^{i+1} \quad (30)$$

$$V_m^{i+1} = \psi * V_m^i + a_1 * r_1 * \left(Pbest_m^i - Y_m^i \right) + a_2 * r_2 * \left(Gbest^i - Y_m^i \right) \quad (31)$$

Where, V_m is velocity of m^{th} particle, Y_m is position of m^{th} particle, $Pbest^i_m$ is personal best of m^{th} particle, $Gbest$ is global best, ψ is weight of inertia, a_1 and a_2 are acceleration coefficient, r_1 and r_2 are random numbers, and i is iteration number. The objective function is defined as the fitness function for the PSO problem, as shown in equation (1). The constraints function for observability is bounded by the equations (2-4). The initialization is started by setting the PSO parameters (weight of inertia, acceleration coefficients, and random number) according to the problem's convenience. Every iteration, the fitness function is evaluated for the specified number of particles. Particle with the lowest fitness value among all particles is chosen as the global best particle. The particle's individual best is defined as the fitness function values for each particle in a given iteration. The particle positions will modify with each iteration in an attempt to achieve their minimum global positions. In the existing optimization process, the particles are referred to as PMUs. There are several optimization method to solve the complex problem (Wong, Shareef et al. 2014)

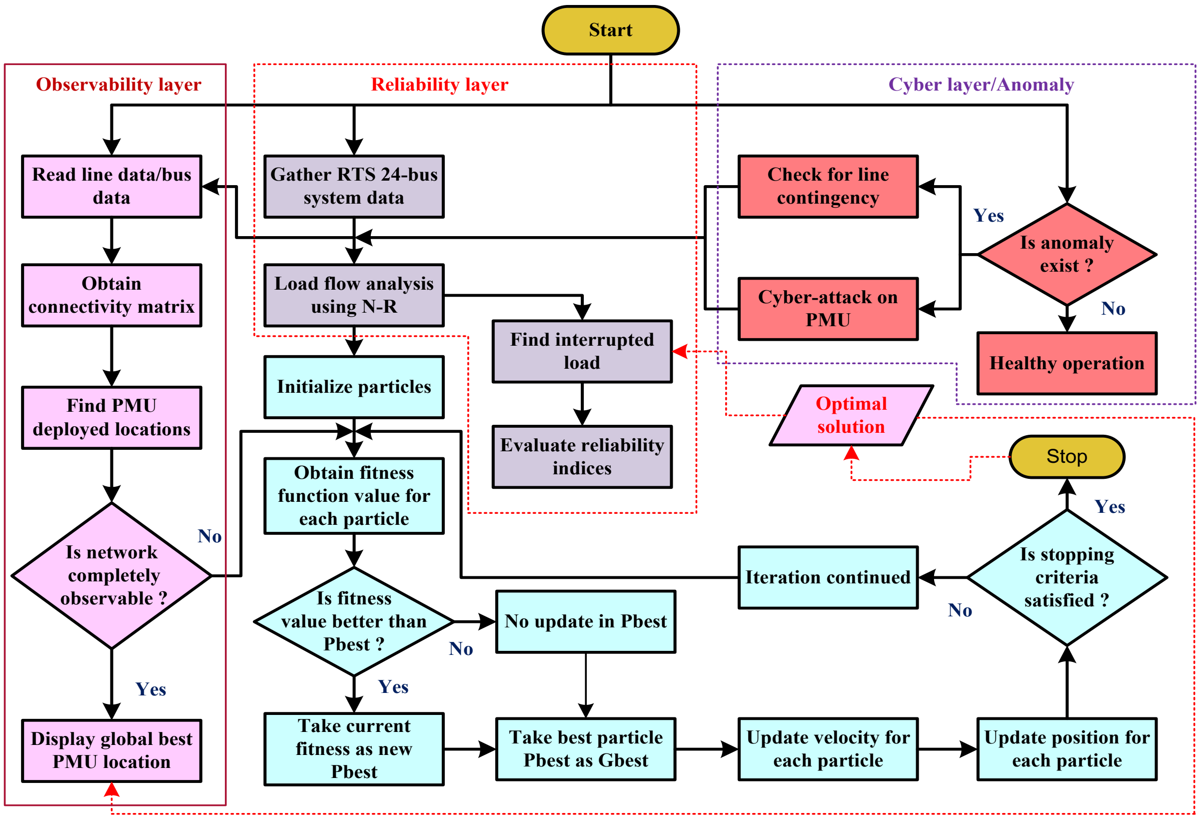

FIGURE 3. Flow chart for evaluation of reliability and observability using PSO Algorithm

CYBER-ATTACK RISK MODEL OF SYNCHROPHASOR NETWORK

PMUs are becoming more vulnerable to cyber risk as they are rapidly integrated into the conventional grid for real-time information of power system parameters.There are many types of cyber-attacks affecting the synchrophasor network. Distributed Denial of Service (DDoS) attacks on the synchrophasor network can take the PMU down. Therefore, there will be no information exchange for PMU measurements (Hampannavar, Swapna et al. 2022). This could cause incomplete information on grid parameters. Thus, the observability of the system becomes more affected during DDoS attacks. Man-in-the-Middle (MITM) attacks occur in the synchrophasor network between the measurement devices PMU and PDC. The attacker gets involved in-between the two devices and disguises themselves as a PMU device for communication with the PDC device and vice-versa. Therefore, an attacker can introduce malicious data into any measurement device to alter its working functionalities. Data spoofing attacks can monitor the measurement data of PMUs as well as their time-stamps. Therefore, the continuous data obtained by PDC may be fabricated data. All these attacks are affecting the PMU operation, so that system observability and reliability need to maintain during such anomalies scenarios (Hettiarachchige-Don, Manoharan et al. 2018, Kholidy 2021). Thus, the challenging task is how to deploy the PMUs in synchrophasor networks during a cyber-attack to retain the observability and reliability. This paper initialises the step towards the optimal PMU deployment in the synchrophasor network during anomalies with the PMU devices. A probabilistic-based method is integrated to analyse the reliability of the synchrophasor network during PMU failure. The backup PMU deployment strategy will move towards the complete observability of the grid network during the cyber-attacks on the PMU devices. The state probability of measurements unit provides the most reliable PMU allocated buses in the system.

PMU state analysis can be defined as shown in equation (32).

$$S_p = \begin{cases} 1, & If\ \ PMU\ \ p\ is\ \ healthy \\ 0, & If\ \ anomaly\ exist\ \ with\ PMU\ \ p \end{cases} \tag{32}$$

Where, for a given set of PMU P, such that $p \in P$, the PMU state is represented as S_p. Let H_s^{pmu} is representing the set of healthy PMUs in the network for observation, UH_s^{pmu} is representing the unhealthy set of PMUs affected due to cyber intrusion in the system. $H_s^{pmu} = \{k : S_k = 1 \mid S\}$ is condition for set of healthy PMUs and $UH_s^{pmu} = \{k : S_k = 0 \mid S\}$ is condition for set of unhealthy PMUs due to cyber-attack. Where, $S = \{S_1, S_2 ...., S_{np}\}$ is set of all the PMU states, is number of PMU in the system. The state probability of PMUs during healthy and unhealthy conditions depends on the Forced Outage Rate (FOR) of the individual PMU during cyber-attack. FOR is also known as the unavailability rate of the PMUs. The state probability of PMUs can be represented by mathematical equation (33). Where, FOR_p and FOR_k is forced outage rate or unavailability rate for p^{th} healthy PMU and k^{th} unhealthy PMU respectively. The objective function gets modified during the cyber-attack with the integration of the state of PMUs. The constraints also follow the inclusion of a PMU state during anomaly conditions with PMUs.

$$\Pr_{st} = \prod_{p \in H} \prod_{k \in UH} \left(1 - FOR_p\right) * \left(FOR_k\right) \quad (33)$$
$$\forall\, p \in H_s^{pmu} \;, k \in UH_s^{pmu}$$

The equations (34–36) represent the modified test system objective during the cyber-attack on the PMU buses. The rest of the other observability and load flow constraints will be similar to previous scenarios when there was no cyber intrusion in the system.

$$Min \quad \sum_{b=1}^{Nb} CV_b^{pmu} * x_b * S_p + \sum_{b=1}^{Nb} LC_b * CV_b^{li} \quad (34)$$

Modified observability constraint: subjected to-

$$O_b \geq 1 \quad \forall b \in B, \; p \in P \quad (35)$$

$$O_b = \sum_{i=1}^{Nb} f_{bi} * x_i * S_p + \sum_{i=1}^{Nb} f_{bi} * y_{bi} \quad (36)$$
$$\forall b \in B, \; p \in P$$

TEST SYSTEM DESCRIPTION

A case study has been performed on the RTS-79 IEEE 24-bus system; it is a conventional power system network (Subcommittee and systems 1979). The network is modified into a synchrophasor network by deploying the measurement devices on the network. The complete network observation is achieved by optimizing the number of PMU installations in the network. The objective function uses cumulative optimization to secure the observability and reliability of the synchrophasor grid system. The whole system is divided into three zones of operation for the study of backup PMU installations in the network during anomaly events that occur on PMU buses due to cyber threats. Each zone is occupied with a backup PMU such that the complete state's observation can be achieved with this backup PMU during abnormalities that occur on the PMU due to an attacker. Figure 4 shows the illustration of a bus diagram for a synchrophasor network, which consists of a 24-bus system and its zone representation. The system consists of four ZIBs located at buses 11, 12, 17, and 24. These buses are neither connected with generators nor loaded. The case study involving the inclusion of ZIB in the objective of the paper is to optimize the total number of PMU requirements in the network for complete state analysis. Table 2 shows the simulation data required for achieving the objective of the paper. The data consists of the installation cost of PMU (in $), penalty charge during load interruption (in $/MW), and PMU availability rate is used to find the state probability. The data on PMU installation costs is applicable to finding the optimal location of PMU devices across the synchrophasor network. The effect of cost is secondary; the observability of the complete network is the primary concern in objective modelling. As a result, whatever the values of the PMU installation cost are, they will only change the objective function values, but the allocation of PMU deployment will remain the same. The reliability of the network is not affected by any cost values of the PMU installation. The penalty data during load interruption at each bus is mentioned to get the load curtailment during unwanted situations like transmission line outages and PMU unhealthy conditions due to cyber intrusion. The PMU availability rate is useful to get the forced outage rate of each PMU's associated buses, which can be modelled for the reliability analysis of the synchrophasor grid during anomalies.

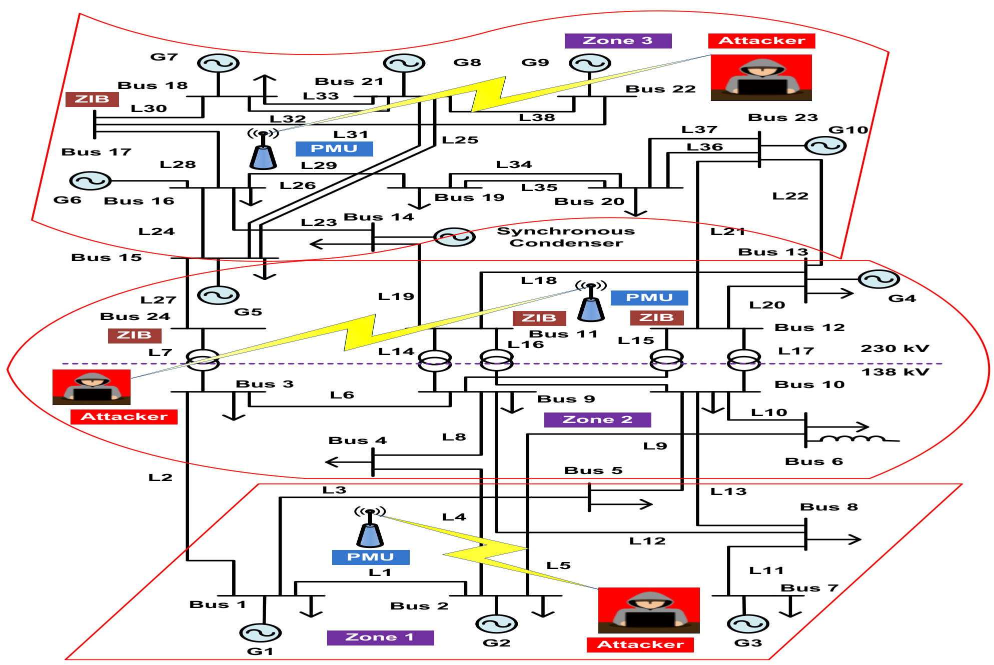

FIGURE 4. Bus diagram illustration of three-zone distribution of RTS-79 IEEE-24 Bus synchrophasor grid test system

TABLE 2. Simulation data for PMUs installation cost, unavailability rate and penalty rate over load interruption in RTS-79 (IEEE 24 bus system)

Bus Number	Bus 1	Bus 2	Bus 3	Bus 4	Bus 5	Bus 6	Bus 7	Bus 8
PMU Installation cost (In $)	32,000	28,000	20,000	22,000	33,500	30,300	27,000	26,700
Penalty on IL (In $/MW)	2.35	2	1.3	8.5	7.6	5	12.5	7.2
PMU Availability rate	0.98	0.99	0.916	0.957	0.982	0.93	0.963	0.99
Bus Number	Bus 9	Bus10	Bus 11	Bus 12	Bus 13	Bus 14	Bus 15	Bus 16
PMU Installation cost (In $)	35,000	18,000	23,700	26,100	29,300	27,300	31,900	20,200
Penalty on IL (In $/MW)	4.12	7.46	3.8	4.8	10.5	8.3	6.86	6
PMU availability rate	0.974	0.963	0.991	0.987	0.975	0.96	0.958	0.97
Bus Number	Bus17	Bus 18	Bus 19	Bus 20	Bus 21	Bus 22	Bus 23	Bus 24
PMU Installation cost (In $)	24,600	28,000	23,500	25,900	20,500	28,400	22,000	21,500
Penalty on IL (In $/MW)	11.5	9.8	9.2	7.6	4.5	5	8.36	7.5
PMU Availability rate	0.946	0.976	0.935	0.919	0.95	0.99	0.96	0.982

The reliability modelling of the system is obtained with the integration of the unavailability of PMU devices due to cyber threats. The test system combined the analysis of observability with the optimum number of PMU deployments in the network and reliability with optimizing the load interruption during several contingencies, such as line contingency and PMU failure due to cyber threats. The reliability of the synchrophasor network is evaluated through the reliability indices ILPI and EDNS during the line contingency, and abnormalities occur with PMU devices due to cyber-attacks. The other data related to this paper, like generator data, line data, and bus data, is taken from the conventional RTS-79 IEEE 24-bus system.

RESULTS AND DISCUSSION

This section simulates the results of the test system for the complete observability of the network along with the most reliable mapping during anomalies with the PMU devices due to cyber-attacks. Using the PSO technique, the optimal value of the objective function results in the cumulative effect of system reliability and observability. Cyber threats have become a more focused area for modelling the synchrophasor network. Therefore, backup deployment of PMU in the system in accordance with the individual failure of the measurement unit can make the system more reliable. The state probability of an individual's failed measuring unit can be obtained with the availability and unavailability of these devices. With this observation, reliability indices can be calculated by merging the effect of cyber-attacks over the communication link installed between the measuring devices. The effect of ZIB is also discussed in optimal placement of PMU with consideration of several contingencies, such as line contingency and the contingency that occurs with measurement devices in the network. The simulation results of the optimum solution for the synchrophasor network observation are discussed in the below subsection.

OPTIMAL PMU DEPLOYMENT IN SYNCHROPHASOR GRID NETWORK WITH AND WITHOUT CONSIDERATION OF ZIB

The test system used for the analysis of the optimal deployment of PMU consists of 24-bus having four zero injection buses 11, 12, 17, and 24. All these ZIB connected with neither load nor generator. Therefore, the inclusion of the effect of such buses results in fewer PMU requirements for the complete observability of the grid. If there exists less number of PMU in the system then the cyber threats to the communication channels will be lesser, which may improve the system reliability. Figure 5 shows the optimal deployment of PMU in the RTS-79 IEEE 24-bus system by considering the effect of ZIB. The optimal number of PMUs required for full observation of the system is six. The location of PMU deployment has been obtained on buses 1, 2, 8, 16, 21, and 23 with the inclusion of the effect of ZIB.

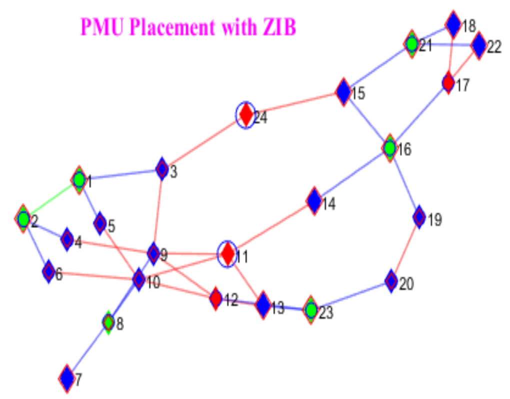

FIGURE 5. PMU deployment in RTS-79 by considering the effect of ZIB, PMU deployed bus (green colour), ZIB (red colour), Line connected to a PMU bus (blue colour), Line connected to two PMU bus (green colour), Line not connected to PMU bus (red colour)

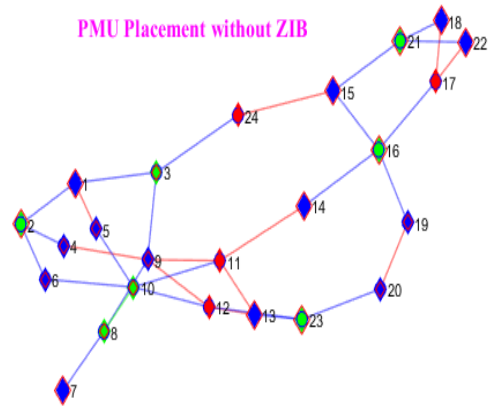

FIGURE 6. PMU deployment in RTS-79 without consideration of ZIB, PMU deployed bus (green colour), ZIB (red colour), Line connected to a PMU bus (blue colour), Line connected to two PMU bus (green colour), Line not connected to PMU bus (red colour)

There will be some lines installed with PMU at both ends, some lines with one end PMU, and some lines missing PMU allocation at either of their ends. However, all these buses are indirectly observable through other PMU bus or ZIB. Figure 6 shows the optimal number of PMU allocations in the RTS-79 IEEE-24 bus synchrophasor system by excluding the effect of ZIB in the observation. Now, by doing so, the optimal number of PMUs required for complete observation of the network is seven. In this scenario, the PMU located at the bus 2, 3, 8, 10, 16, 21, and 23 makes the system observable. Thus, PMU location is changing by including or excluding the effect of ZIB in the network. Now, the new buses 3 and 10 have PMU installation, excluding the effect of ZIBs. The results of the study indicate that the inclusion of ZIB in the system can reduce the total number of PMUs required in the synchrophasor network.

EFFECT OF TRANSMISSION LINE SWITCHING OVER THE OPTIMAL PMU DEPLOYMENT WITH AND WITHOUT CONSIDERATION OF ZIB

Effect of Line Contingency with Inclusion of ZIB

Transmission line switching is commonly used to analyse the reliability of conventional power systems by optimising load curtailment while observing load demand and power flow in transmission lines. The integration of synchrophasor measurements devices into the conventional power system makes the system smarter, but maintaining the reliability is the focus of research in the field of smart grid reliability. This paper includes the cumulative optimization of reliability and observability. Therefore, during line contingency, it may cause an increment in the number of PMU requirements in the system for complete observation. Thus, the optimum cost function will be different with different line contingencies. As the number of PMU required for the test system is six, considering the effect of ZIB. The objective of the cost function results in an optimum value of 154,628.02 (in $) in base case scenarios when there is no contingency in the grid network. The RTS-79 IEEE 24-bus system consists of 38 transmission lines, thus simulating each line's contingency effect over the requirement for the optimal number of PMUs and its location is shown in the Table 3.

There is an eight-line contingency that requires seven PMU instead of six PMU (base case) for the complete overview of the states of the network. Those line contingencies are numbered as L2, L3, L4, L5, L11, L12, L13, and L29.

TABLE 3. Transmission line switching effect over the deployment of PMUs with consideration of ZIB

Line Contingency	Bus number with PMU location (With ZIB)	Optimal total number of PMUs	Optimal objective function value (In $)	Time for computation (sec)
Base Case	1, 2, 8, 16, 21, 23	6	154628.02	1.7819
L2	2, 8,9, 10, 16,21, 23	7	176416.75	1.8273
L3	2, 8,9, 10, 16,21, 23	7	177912.62	1.7732
L4	1, 8,9, 10, 16,21, 23	7	181596.86	1.8826
L5	1, 8, 9,10, 16,21, 23	7	180773.10	1.7461
L11	2, 7, 9,10, 16,21, 23	7	176741.05	2.0341
L12	1, 8,9, 10,16, 21, 23	7	182048.40	1.8789
L13	1, 8,9, 10,16, 21, 23	7	179985.12	1.8961
L21	1, 2, 8, 13, 19, 21	6	165432.03	1.7388
L22	1, 2, 8, 13, 19, 21	6	167254.28	1.8323
L23	1, 2, 8, 13, 19, 21	6	165825.00	1.7459
L28	1, 2, 8, 13, 19, 21	6	166392.57	1.7457
L29	2, 8, 9,10, 16,20, 21	7	182633.25	1.9105

:- The list of remaining line contingency have PMU location at the bus 1, 2, 8, 16, 21, 23 similar to base case, although optimal objective function value and computational time are different in such scenarios.

Out of 38-line contingencies, 12 such contingencies will change the location of the PMU deployed bus with respect to the base case. All these twelve-line contingencies are listed in Table 3.

Out of these twelve, four-line contingencies (L21, L22, L23, and L28) required a total of six PMU for full observability of the grid test system. In all these four-line contingency scenarios, the total number of PMU requirements is similar to the base case, i.e., six, but the location of the PMU deployment bus number is subject to change. The rest of the remaining line contingency has similar characteristics for PMU location as mentioned in the base case. For these line contingencies, the optimal objective function value may be changed because it depends on the load interruption cost during the contingency, although the PMU installation cost is similar to the base case. The inclusion of ZIB characteristics results in a lower number of PMUs required for the complete state analysis of the grid network. The highest cost value was obtained with the L29 line contingency, resulting in a cost of 182,633.25 (in $).The total increment in cost is 18.11% during the transmission line switching of L29, observing the base case scenarios.

Effect of Line Contingency with Exclusion of ZIB

The specified test system can be optimally observable with seven PMU by excluding the effect of ZIB in the network. This base case PMU allocation can be used to compare the line contingency effect over the PMU deployment in the synchrophasor network. As the requirements of the total number of PMU are increased to seven by excluding the effect of ZIB, As a result of the twelve-line contingency, the topology of PMU placement in the network is changed as shown in Table 4. There are nine such line contingencies that require a total of eight PMU for the full state's observation. These lines of contingency are numbered as L4, L7, L9, L16, L22, L23, L28, L29, and L38. The line contingency L1, L2, and L11 required seven PMUs in the network, similar to the base case, but the location of placement of all these PMUs is different from the base case scenarios. The remaining 26 lines of contingency out of 38 have similar characteristics for PMU deployment. This line contingency may not change the topological view of the network, but it will change the objective function value due to the change in load interruption that occurs with each line contingency. In the base case scenarios, the optimum cost is obtained at 162,087.62 (in $).

TABLE 4. Line contingency effect over the deployment of PMUs without consideration of ZIB

Line Contingency	Bus number with PMU location (Without ZIB)	Optimal total number of PMUs	Optimal objective function value (In $)	Time for computation (sec)
Base Case	2, 3,8, 10, 16,21, 23	7	162087.62	1.9030
L1	3, 4, 8, 10, 16, 21, 23	7	155712.34	2.1860
L2	2, 8, 10,16, 21, 23, 24	7	163241.38	1.9549
L4	1, 3, 8,9, 10,16, 21, 23	8	204286.02	2.2010
L7	2,8,9,10,15,16,17,23	8	212829.35	2.1360
L9	1, 8,9,10, 15,16, 21, 23	8	213627.19	2.1322
L11	2, 3, 7, 10, 16, 21, 23	7	160971.73	2.0459
L16	1, 3, 8, 9,10, 16, 21, 23	8	199638.87	1.8546
L22	2, 8, 9,10,11,15, 17, 20	8	221078.62	2.0869
L23	1,8, 9,10,11, 15, 17, 20	8	224332.17	1.8701
L28	1,8, 9, 10,15, 16,17, 23	8	216726.94	1.9173
L29	1,8, 9, 10,11, 15,17, 20	8	223963.02	2.2010
L38	1,8, 9, 10,15, 16,17, 23	8	215489.71	2.1420

:- The list of other line contingency have PMU location at the bus 2, 3, 8, 10, 16, 21, 23 similar to base case, although optimal objective function value and computational time are different in such scenarios.

The contingency occurs with line one (L1) results in the optimal value of the cost function equal to 155,712.34 (in $). The cost value is reduced by 3.93% by considering the line contingency L1 with respect to the base case observation. The highest cost value obtained is equal to 224,332.17 (in $) during line switching of L23. In this case, the cost value increased 38.4% by observing the base case.

BACKUP OPTIMUM PMU ALLOCATION DURING ANOMALY WITH MEASUREMENTS DEVICES DUE TO CYBER-ATTACK BY INCLUDING THE EFFECT OF ZIB

The present power system network integrated with synchrophasor measurements devices affects the reliability of the grid network during cyber-attacks. The loss of PMU devices or their communication channels results in an unreliable network topology. Therefore, backup PMU modelling in the existing synchrophasor grid may lead to greater reliability of the system during anomalies with any measurement device. The backup PMU installation is presented by including the effect of ZIB in the network. Initially, six PMU-deployed buses exist in the network for the entire state's observation, including the effect of ZIB. This scenario is used for a comparative study of the backup PMU location during cyber-attacks. The test system is divided into three zones to provide the backup PMU for a particular zone during the failure of any zone PMU due to cyber threats. In the base case, buses 1, 2, and 8 of the first zone and buses 16, 21, and 23 of the third zone are occupied by PMU. There are no PMUs that exist in the second zone of the test system, although the network is completely observable. During abnormity with PMU located at bus-1 of the first zone due to a cyber-attack, the backup PMU deployment would be used for complete state analysis of the network. The anomaly occurs on bus 1, resulting in the new PMU location at buses 1, 6, 8, 9, 10, 16, 21, and 23 for complete observations. Therefore, a remedy for complete state observability due to PMU failure at bus-1 is maintained by installing the backup PMUs at buses 6, 9, and 10 of the second zone. Figure 7 shows the backup modelling of PMUs' placement during an anomaly, with zone one PMU located at bus-1. During the failure of the PMU located at bus-2 in the first zone, the new observation can be obtained by placing the PMU at buses 2, 3, 8, 9, 10, 16, 21, and 23.

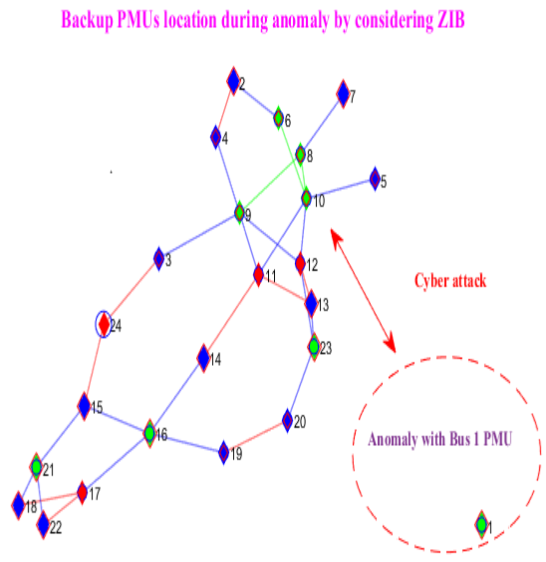

FIGURE 7. Backup modelling of PMUs deployment during anomaly with PMU located at bus 1 considering ZIB, PMU located bus (green), ZIB (red), Line connected to a PMU bus (blue), Line connected to two PMU bus (green), Line not connected to PMU bus (red)

TABLE 5. Zone wise distribution of backup PMUs during anomaly with PMU deployed bus considering ZIB

Anomaly exist with bus PMU during attack	Zone 1		Zone 2		Zone 3	
	PMU bus without any anomaly	Bus with backup PMU	PMU bus without any anomaly	Bus with backup PMU	PMU bus without any anomaly	Bus with backup PMU
At Bus 1	1, 2, 8	1, 8	-	6, 9, 10	16, 21, 23	16, 21, 23
At Bus 2	-	2, 8	-	3, 9, 10	-	16, 21, 23
At Bus 8	-	1, 7, 8	-	9, 10	-	16, 21, 23
At Bus 16	-	1, 2, 8	-	13	-	16, 20, 21
At Bus 21	-	1, 2, 8	-	-	-	16, 17 21, 23
At Bus 23	-	1, 2, 8	-	11	-	19, 21, 23

Therefore, the backup PMU required to prevent the system's observability and reliability should be installed on buses 3, 9, and 10 of the second zone. The backup PMU required in the grid network during a cyber-attack on the PMU located at bus-8 of the first zone should be installed at bus-7 of the first zone and buses 9, and 10 of the second zone for full observation of the states. The backup PMU should be installed at bus-13 in the second zone and bus-20 in the third zone to maintain the observability of the network during an anomaly, which exists with the PMU located at bus-16 in the third zone. Similarly, the backup PMU should be deployed on bus 17 of the third zone for complete state observation during a cyber-attack on bus 21 of the third zone. Two backup PMUs are required during an anomaly with the PMU located at bus-23 in the third zone. They should be placed at bus-11 in the second zone and bus-19 in the third zone. Table 5 shows the zone wise distribution of backup PMUs during cyber-attack on the existing PMU with consideration of ZIB in the system.

BACKUP OPTIMUM DEPLOYMENT OF PMU DURING ANOMALY WITH MEASUREMENTS DEVICES DUE TO CYBER-ATTACK BY EXCLUDING THE EFFECT OF ZIB

As for excluding the effect, ZIB can increase the number of PMUs required for a complete state analysis of the network. The backup PMU modelling is simulated for reliability and observability analysis of the network by excluding the effect of ZIB. Initially, buses 2, and 8 of the first zone, buses 3, and 10 of the second zone, and buses 16, 21, and 23 of the third zone are occupied with the PMU by excluding the effect of ZIB. If there is a cyber-attack on bus 2 in the first zone, the backup PMU should be placed on bus 9 in the second zone. Further, if a cyber-attack causes any abnormalities on bus-3 of the second zone, the optimal backup PMU location is obtained at buses 2, 3, 8, 10, 15, 16, 17, and 23 to fulfil the objective criteria. The backup PMU location is obtained at buses 15, and 17 in the third zone during the anomaly with bus-3. Similarly, if the PMU at bus-8 in the first zone is affected by cyber intrusion, then the new location of the PMU should be placed at 2, 3, 7, 8, 10, 16, 21, and 23. Therefore, the backup PMU installation can take place at bus-7 in the first zone. Figure 8 shows the backup PMU allocation modelling during a cyber-attack that occurs at bus-10. By observing the results, a backup PMU should be placed at bus-1 of the first zone, bus-9 of the second zone, and bus-15 of the third zone for complete state observability during an anomaly, with a PMU installed at bus-10. The backup PMU placed at bus-1 of the first zone, bus 9, and 11 of the second zone, bus 15, 17, and 20 of the third zone can ensure the system observability during the cyber-attack that takes place at bus-16 PMU. Similarly, deploying a backup PMU at bus-17 can make the system states observable when an anomaly occurs with the PMU allocated at bus-21. Further, if there are abnormalities with PMU allocated to bus 23, the new placement of PMU takes place on buses 2, 8, 9, 10, 11, 15, 17, 19, and 23. Therefore, observability of the system can be ensured with the installation of backup PMU on buses 9, and 11 in the second zone, and buses 15, 17, and 19 in the third zone. Table 6 shows the zonal distribution of backup PMU during an anomaly occurs with the existing deployed PMU by excluding the effect of ZIB.

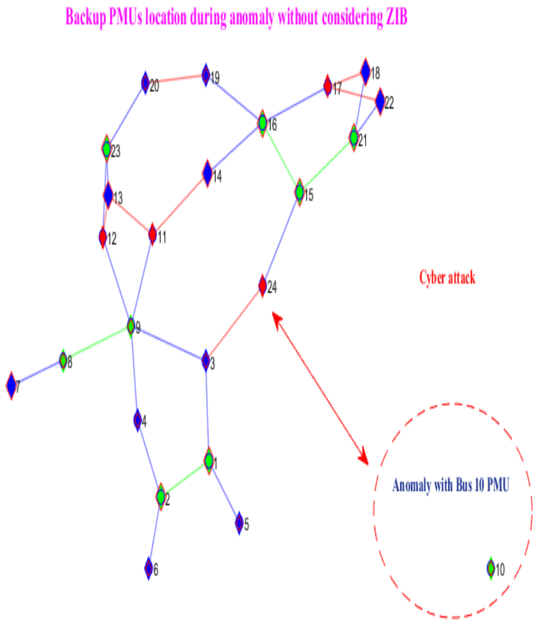

FIGURE 8. Backup modelling of PMUs deployment during cyber-attack on PMU located at bus 10 without considering ZIB, PMU located bus (green), ZIB (red), Line connected to PMU bus (blue), Line connected to two PMU bus (green), Line not connected to PMU bus (red)

STATE PROBABILITY TABLE FOR THE PMU UNAVAILABILITY DURING ANOMALY WITH MEASUREMENT DEVICES

The state probability of PMU availability and unavailability are calculated with the inclusion and exclusion of ZIB in

TABLE 6. Zone wise distribution of backup PMUs during anomaly cause by cyber-attack over the PMU deployed bus without considering the effect of ZIB

Anomaly exist with bus PMU during attack	Zone 1		Zone 2		Zone 3	
	PMU bus without any anomaly	Bus with backup PMU	PMU bus without any anomaly	Bus with backup PMU	PMU bus without any anomaly	Bus with backup PMU
At Bus 2	2, 8	2, 8	3, 10	3, 9, 10	16, 21, 23	16, 21, 23
At Bus 3	-	2, 8	-	3, 10	-	15,16, 17, 23
At Bus 8	-	2, 7, 8	-	3, 10	-	16, 21, 23
At Bus 10	-	1, 2, 8	-	9, 10	-	15,16, 21, 23
At Bus 16		1, 8		9, 10,11		15,16, 17, 20
At Bus 21	-	2, 8	-	3, 10	-	16,17, 21, 23
At Bus 23	-	2, 8	-	9, 10,11	-	15,17, 19, 23

the grid network. There exist six PMU for complete states observation of the test system considering the effect of ZIB. If all the PMUs of the system are in healthy condition, means there is no cyber intrusion; the state probability of all available PMU can be obtained by multiplying the availability rate of each PMU. If any one of the PMU gets affected by a cyber-attack, the state probability of cumulative outage of one PMU can be obtained by summing the state probability of each individual PMU outage. The state probability of failure of a single PMU is calculated by multiplying the availability rate of all-available PMU and Forced Outage Rate (FOR) or unavailability rate of a single PMU outage. The sum of availability rate and unavailability rate of a PMU is always equal to one. Therefore, if the availability rate of a PMU is known then the unavailability rate for the PMU can be obtained. Similarly, all the possible combinations of two PMU failures in the system can be calculated. Thus, by doing so, the state probability table of PMU availability and unavailability can be obtained in both the scenarios i.e. with and without consideration of ZIB. Table 7 shows the state probability of PMU failure due to cyber-attack.

TABLE 7. State probability table of PMUs unavailability during anomaly due to cyber-attack

With Consideration of ZIB			Without Consideration of ZIB		
PMU Available	PMU Unavailable	State Probability	PMU Available	PMU Unavailable	State Probability
6	0	0.84969495	7	0	0.76481910
5	1	0.14091024	6	1	0.21074801
4	2	0.00909955	5	2	0.02308869
3	3	0.00029043	4	3	0.00130291
2	4	0.00000479	3	4	0.00004060
1	5	0.00000004	2	5	0.00000069
0	6	0.0000000001	1	6	0.00000001
-	-	-	0	7	0.00000000

RELIABILITY ANALYSIS OF SYNCHROPHASOR SMART GRID SYSTEM DURING ANOMALY WITH PMU BY CONSIDERING THE EFFECT OF ZIB

Synchrophasor measurements technology is rapidly integrating into the traditional power network for more accurate real-time grid observation. The communication channels connecting the measuring devices to the control center are more vulnerable due to cyber intrusion in the system. Therefore, the failure of PMU during attacks can make the system unobservable, and the unhealthy condition of PMU may affect the reliability of the system. The reliability indices ILPI and EDNS are evaluated during the cyber-attacks that occur on the PMU-located bus. With the inclusion of ZIB in the network, the optimal number of PMU requirements for complete state observation is equal to six. These buses are deployed on buses 1, 2, 8, 16, 21, and 23. Now, ILPI is being evaluated for each PMU failure due to cyber-attacks. Figure 9 shows the reliability parameter ILPI during anomaly occurs with the existing PMU in the given scenarios. The anomaly that occurs with PMU deployed at bus 1, 2, and 8 affects the network more strongly in comparison with cyber-attacks that occur at bus 16, 21, and 23. Therefore, the network becomes more reliable whenever the cyber-attack occurs at buses 16, 21, and 23 in comparison with the reliability of the network affected due to abnormalities occurring at buses 1, 2, and 8. System reliability will be improved by minimizing the values of reliability indices such as ILPI and EDNS. The reliability parameter ILPI gets reduced by 20.52% during a cyber-attack that occurs at bus-2, observing the ILPI value during the cyber-attack at bus-1. The reliability parameter ILPI increased by 38.29% during the anomaly that occurred at bus-8, observing the reliability index during the cyber-attack at bus-1. Similarly, the reliability parameter ILPI gets reduced by 98.5%, 99.98%, and 98.21% during cyber-attacks that occur at PMU located on buses 16, 21, and 23, respectively, observing the index value during the anomaly with bus-1. Therefore, the reliability of the network will be more affected due to cyber-attacks occurring at PMU allocated buses 1, 2, and 8. Similarly, other reliability parameters such as EDNS can be calculated for each PMU failure due to cyber threats. Figure 10 shows the mapping of reliability index EDNS during a cyber-attack on PMU buses. By considering the PMU failure at bus-1 due to a cyber-attack as the base case, the comparative analysis of reliability for other PMU failures is obtained. The reliability index EDNS is reduced by 10.35% during an attack that occurs at PMU allocated to bus-2, observing the base case scenarios. Similarly, the reliability parameter EDNS is increased by 63.44% when an anomaly occurs with PMU deployed at bus-8 observing the base case index obtained during the attack at bus-1. Similarly, the reliability parameter EDNS is reduced by 99.07%, 99.9%, and 98.74% during cyber-attacks that occur at PMU allocated bus 16, 21, and 23, respectively. The concluding remarks of the observation are that the system will remain in a reliable situation during a cyber-attack that occurs at PMU deployed buses 16, 21, and 23. On the other hand, the system reliability will be more affected due to the cyber-attacks that occurred on buses 1, 2, and 8. If the reliability index is either ILPI or EDNS, a cyber-attack occurs at bus k are denoted by RI_k then by this notation, the reliability index for PMU deployed at bus can be represented in descending order as:

$$RI_8 > RI_1 > RI_2 > RI_{23} > RI_{16} > RI_{21}$$

The above observation is showing that the reliability index for anomaly occurs with PMU deployed at bus-8 is higher in comparison with other PMU deployment in the system. Therefore, the system becomes less reliable in case of abnormalities occurs with bus-8. The reliability index is lesser for bus-21 PMU in comparison with other existing PMU in the system therefore; system becomes more reliable during failure of PMU deployed at bus-21. On the other hand, failure of PMU allocated at bus-21 will not much affect the reliability of the system. The system will be more reliable if its reliability parameter values will be lesser.

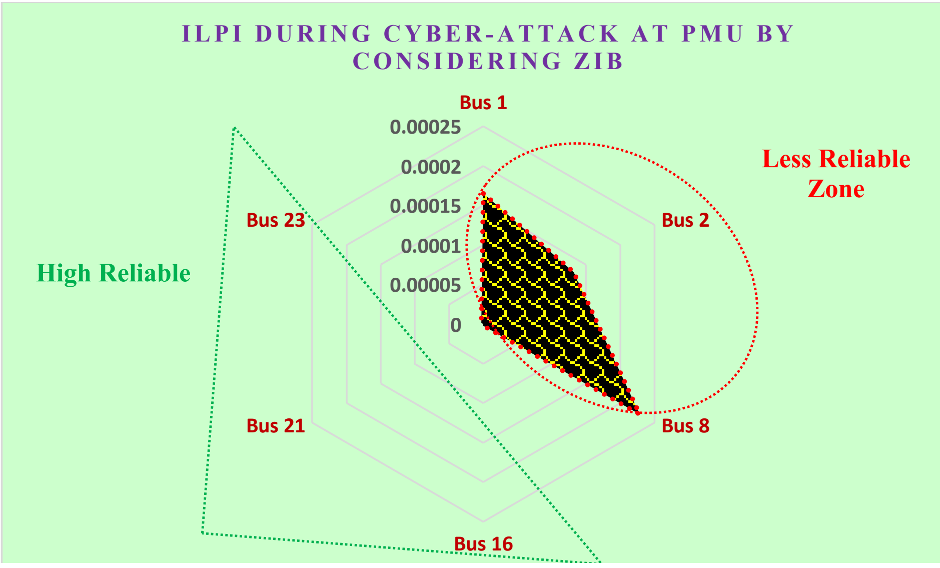

FIGURE 9. Reliability parameter ILPI mapping during cyber-attack at PMU buses with consideration of ZIB

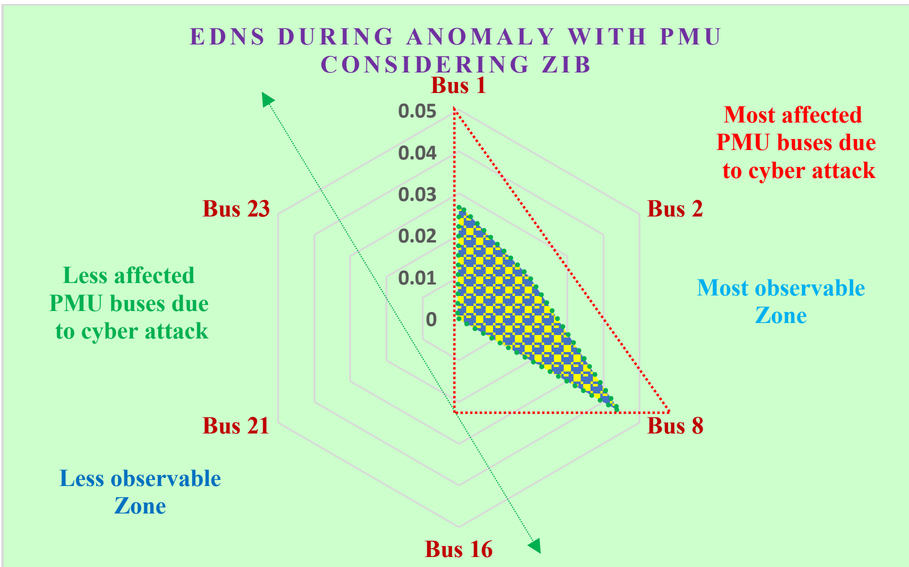

FIGURE 10. Reliability parameter EDNS mapping during cyber-attack at PMU buses with consideration of ZIB

RELIABILITY ANALYSIS OF SYNCHROPHASOR SMART GRID SYSTEM DURING ANOMALY WITH PMU DUE TO CYBER THREATS BY EXCLUDING THE EFFECT OF ZIB

By excluding the effect of ZIB, the total number of PMUs required for complete observation of the network is equal to seven. This PMU is deployed on system buses 2, 3, 8, 10, 16, 21, and 23. The reliability test of such a system can be obtained by considering the cyber intrusion into the grid network. For the analysis of synchrophasor network reliability, the reliability parameters ILPI and EDNS have been evaluated. Figure 11 shows the mapping of reliability index ILPI during cyber-attack that occurs on PMU buses. The most reliable case will be obtained during the anomaly with PMU deployed on buses 2, 3, 8, 10, and 21. The reliability of the network will be highly affected during the cyber-attack that occurs at PMU on buses 16, and 23. By considering the ILPI value obtained during the anomaly with bus-23 as a base case, the comparative analysis of reliability during the failure of other bus PMUs is evaluated.

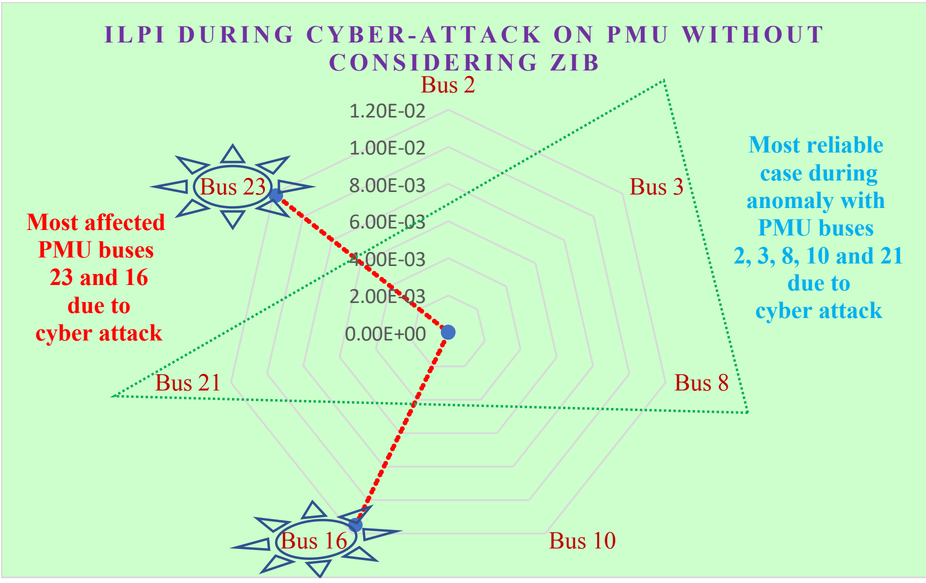

FIGURE 11. ILPI mapping during anomaly due to cyber-attack at PMU buses without considering ZIB

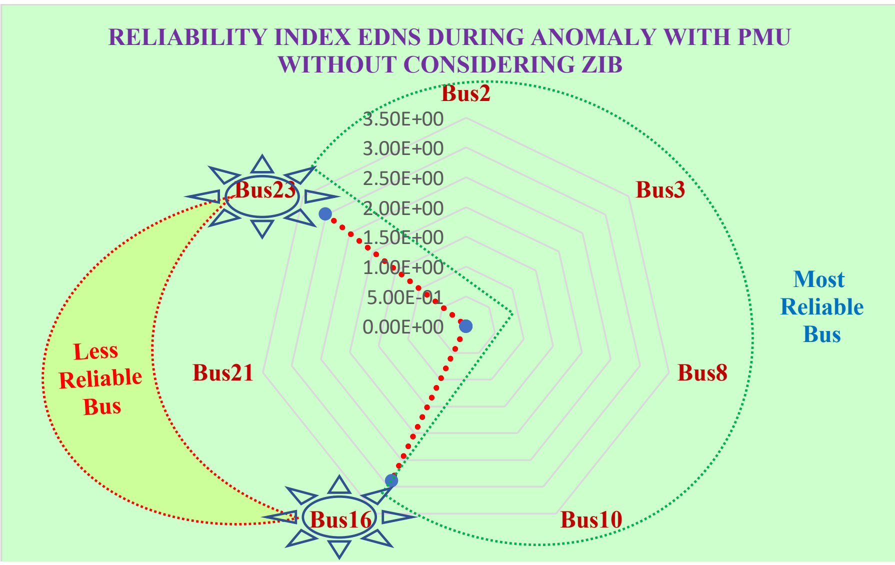

FIGURE 12. Reliability index EDNS mapping during cyber-attack at PMU buses without consideration of ZIB

During the cyber-attack that occurs at bus-16, the reliability parameter ILPI is reduced by 2.67%, observing the base case scenario reliability index obtained during the anomaly with bus-23. Failure due to cyber intrusion has little impact on system reliability, as the ILPI index is reduced by 99.9% for cyber-attacks that occur at buses 2, 3, 8, and 21, and it is reduced by 99.7% during anomaly with PMU allocated at bus-10 in comparison to base case scenarios. Figure 12 shows the mapping of the reliability index EDNS during an anomaly that occurs at the PMU buses in the network. Similarly, the reliability index EDNS is reduced by 4.5% during a cyber-attack that occurs at bus-16, observing the base case having a failure of PMU deployed at bus-23. The EDNS index is reduced by 99.9% during a cyber-attack that occurs on buses 2, 3, 8, and 21 while observing the base case. Similarly, it reduces 99.8% during an anomaly with PMU allocated to bus-10 by observing the base case scenarios.

$$RI_{23} > RI_{16} > RI_{10} > RI_{3} > RI_{21} > RI_{2} > RI_{8}$$

The reliability index for bus-23 is higher, which means the system becomes less reliable during the failure of the PMU allocated to bus-23. The system network will be more reliable or it will not be affected more when the anomaly occurs at PMU deployed bus-8. The reliability index for each PMU failure due to cyber-attack is represented in descending order as shown below. The concluding remarks of observation are that the higher the reliability index, the less reliable the network will be, and the lower the reliability index, the more reliable the network will be.

CONCLUSION & FUTURE RESEARCH

This paper discusses the cumulative effect of synchrophasor network observability and reliability by optimizing the total number of PMUs deployed and load curtailments that occur during cyber intrusion. The effect of ZIB is integrated with the constraints of observability, which provides the complete state's analysis with a lower number of PMU deployments in the grid network. The backup PMU modelling ensures the system observability and reliability during anomaly events that occur with PMU devices due to cyber-attack. The transmission line switching effect over the PMU placement can be obtained by excluding and including the effect of ZIB. The state probability of PMU availability and unavailability are integrated with the conventional system reliability parameters to analyze the reliability of the synchrophasor smart grid network during abnormalities with measurement devices. The concluding remarks of the paper are to find the optimal allocation of the PMU devices for complete state observation of the synchrophasor network along with the optimization of load interruption during anomaly, which exists with PMU devices in the network. Assessment of the impacts of bad data, which might result from poor quantification testing and calibration or information breakdowns, is an essential approach for future research. If all these impacts were completely disregarded, they may have had a negative impact on reliability. As a result, the PDCs can compute quantification residuals to completely eradicate significant errors.

ACKNOWLEDGEMENT

The authors take such an opportunity to express their greatest appreciation to SVNIT Surat, Gujarat, India, for offering an environment for the research project that allowed us all to make preparations for this manuscript.

DECLARATION OF COMPETING INTEREST

None

NOMENCLATURE

Index and Sets

b	Indexing of buses
gu	Generating unit indexing
tl	Transmission line indexing
c	Contingency indexing
p	PMU indexing
B	Collection of bus indexing
GU	Indexing set of generating units
TL	Collection of transmission lines indexing
C	Collection of contingency indexing
P	Collection of PMU indexing

Variables and parameters

Nb	Total number of buses in the system
CV_b^{pmu}	Cost value of PMU placed at bus b
CV_b^{li}	Penalty cost value on load curtailments at bus b
LC_b	Load curtailments at bus b
O_b	Observability of bus b
f_{bi}	The b^{th} row and i_{th} column entry of connectivity matrix
y_{bi}	Auxiliary variable added at each ZIB
$\Pr_i$	Individual probability
θ_b	Voltage angle of bus b
LF_{tl}	Active power generation capacity of unit gu
Ω_{tl}	Power flow capacity of transmission line tl
LD_b	Binary digit variable
$CN_{b,gu}$	Load demand at bus b

$CN_{b,gu}$	Connection node matrix of bus and generating unit
$IN_{b,tl}$	Incidence node matrix of bus and transmission line
B_{tl}	Electrical susceptance of transmission line *tl*
M	Large number
$J^{\max}$	maximum number of transmission switches that can be switched at the same time
EPR_n	Number of extra PMU requirements
$\Pr_{st}$	State probability of PMU
$ILPI_S^{AP}$	Interrupted load probability index of system during anomaly with PMU
$LOLP_S^{H}$	Loss of load probability of system during healthy operation of PMU
$EDNS_S^{AP}$	Expected demand not supplied of system during anomaly with PMU

REFERENCES

Abdolahi, A., N. Taghizadegan, M. R. Banaei, J. Salehi and Technology. 2021. A reliability-based optimal µ-PMU placement scheme for efficient observability enhancement of smart distribution grids under various contingencies. *IET Science, Measurement.*

Abdulrahman, I. and G. Radman. 2018. ILP-based optimal PMU placement with the inclusion of the effect of a group of zero-injection buses. *Journal of Control, Automation and Electrical Systems* 29(4): 512-524.

Almasabi, S. and J. Mitra. 2019. A fault-tolerance based approach to optimal PMU placement. I*EEE Transactions on Smart Grid* 10(6): 6070-6079.

Almunif, A. and L. Fan .2020. Optimal PMU placement for modeling power grid observability with mathematical programming methods. *International Transactions on Electrical Energy Systems* 30(2): e12182.

Babu, R. and B. Bhattacharyya .2016. Optimal allocation of phasor measurement unit for full observability of the connected power network. *International Journal of Electrical Power Energy Systems* 79: 89-97.

Blair, S., G. Burt, N. Gordon and P. Orr. 2018. Wide area protection and fault location: review and evaluation of PMU-based methods. ICDPSP (International Conference on Developments in Power System Protection), 2018, 1-6.

Chakhchoukh, Y., H. Lei and B. K. Johnson. 2019. Diagnosis of outliers and cyber attacks in dynamic PMU-based power state estimation. *IEEE Transactions on Power Systems* 35(2): 1188-1197.

Deng, X., D. Bian, D. Shi, W. Yao, Z. Jiang and Y. Liu. 2019. Line outage detection and localization via synchrophasor measurement. ISGT Asia (IEEE Innovative Smart Grid Technologies-Asia), 2019, 3373-3378.

Ding, W., M. Xu, Y. Huang, P. Zhao and F. Song. 2021. Cyber attacks on PMU placement in a smart grid: Characterization and optimization. *Reliability Engineering System Safety* 212: 107586.

Edib, S. N., Y. Lin, V. M. Vokkarane, F. Qiu, R. Yao and D. Zhao. 2020. Optimal PMU restoration for power system observability recovery after massive attacks. *IEEE Transactions on Smart Grid* 12(2): 1565-1576.

Fadhilah, A.R., Mahendran, S., Amir, H.H., and Izham, Z.A. 2009. Load forecasting using time series models. *Jurnal Kejuruteraan (Journal of Engineering)* 53-62.

Gholami, M., A. Abbaspour, S. Fattaheian-Dehkordi, M. Lehtonen, M. Moeini-Aghtaie and M. Fotuhi. 2020. Optimal allocation of PMUs in active distribution network considering reliability of state estimation results. *IET Generation, Transmission Distribution* 14(18): 3641-3651.

Hampannavar, S., M. Swapna, B. Deepa and U. Yaragatti. 2022. Micro Phasor Measurement Unit (µPMU) in smart distribution network: A cyber physical system. ICPS (International Conference on Intelligent Cyber-Physical Systems), 2022, 1-10.

Hettiarachchige-Don, A. C. S., A. K. Manoharan, L. G. Pedaprolu and V. Aravinthan. 2018. Assessment of System Reliability in Presence of Cyber Attack Risk on PMU Data. ICIAFS (IEEE International Conference on Information and Automation for Sustainability), 2018, 1-5.

Jimada-Ojuolape, B. 2021. Reliability enhancement of synchrophasor-based DTR system considering N-1 contingency for PMU placement. IFEEC (IEEE International Future Energy Electronics Conference), 2021, 1-6.

Jimada-Ojuolape, B. and J. Teh. 2020. Impact of the integration of information and communication technology on power system reliability: A review. *IEEE Access* 8: 24600-24615.

Jimada-Ojuolape, B. and J. Teh. 2020. Surveys on the reliability impacts of power system cyber–physical layers. *Sustainable Cities Society* 62: 102384.

Jimada-Ojuolape, B. and J. Teh. 2021. Impacts of communication network availability on synchrophasor-based DTR and SIPS reliability. *IEEE Systems Journal*.

Kholidy, H. A. 2021. Autonomous mitigation of cyber risks in the Cyber–Physical Systems. *Future Generation Computer Systems* 115: 171-187.

Kovalenko, P. Y., V. I. Mukhin, M. D. Senyuk and D. D. Kornilova. 2020. Review of Methods for Power Systems State Estimation and Data Validation Based on Synchrophasor Measurements. RTUCON (International Scientific Conference on Power and Electrical Engineering of Riga Technical University), 2020, 1-5.

Kumar, S., B. Tyagi, V. Kumar and S. Chohan. 2018. Incremental PMU placement considering reliability of power system network using analytical hierarchical process. *IET Generation, Transmission Distribution* 12(16): 3900-3909.

Lu, C., Z. Wang, M. Ma, R. Shen and Y. Yu. 2018. An optimal PMU placement with reliable zero injection observation. *IEEE Access* 6: 54417-54426.

Mustafa, H. M., D. Wang, K. Sajan, E. N. Pilli, R. Huang, A. K. Srivastava, J. Lian and Z. Huang. 2021. Cyber-Power Co-Simulation for End-to-End Synchrophasor Network Analysis and Applications. SmartGridComm (IEEE International Conference on Communications, Control, and Computing Technologies for Smart Grids), 2021, 164-169.

Nageswara Rao, A., P. Vijaya Priya, M. Kowsalya and R. Gnanadass. 2019. Wide area monitoring for energy system: A review. *International Journal of Ambient Energy* 40(5): 537-553.

Noureen, S. S., V. Roy and S. B. Bayne. 2017.Phasor measurement unit integration: A review on optimal PMU placement methods in power system. R10-HTC (Region 10 Humanitarian Technology Conference), 2017, 328-332.

Patil, G. C. and A. Thosar. 2017. Application of synchrophasor measurements using PMU for modern power systems monitoring and control. ICCPEIC (International conference on computation of power, energy information and commuincation) 2017, 754-760.

Peng, J., N. Nair and R. Sherry. 2013. Transmission tomorrow: Development of synchrophasor applications in the New Zealand grid. *Australian Journal of Electrical Electronics Engineering* 10(3): 407-416.

Popov, A. I., A. V. Mokeev, S. A. Piskunov and A. V. Rodionov. 2020. Applications of synchrophasor measurement to improve the reliability and efficiency of power systems. E3S (Web of Conferences), 2020, 01045.

Rahman, N. H., A. F. Zobaa and M. Theodoridis. 2015. Improved BPSO for optimal PMU placement. UPEC (International Universities Power Engineering Conference), 2015, 1-4.

sadat Khalafi, Z., M. Dehghani, A. Khalili, A. Sami, N. Vafamand and T. Dragicevic. 2021. Intrusion detection, measurement correction, and attack localization of PMU networks. *IEEE Transactions on Industrial Electronics*.

Subcommittee, P. M. and systems. 1979. IEEE reliability test system. *IEEE Transactions on Power Apparatus* (6): 2047-2054.

Sushma, G. C. and T. Jyothsna 2018. Observability constrained GA approach for optimal PMU placement considering zero injection modeling. ICCPCCT (International Conference on Control, Power, Communication and Computing Technologies), 2018, 174-178.

Vaiman, M., V. Energy and M. Vaiman. 2018. Use of PMU-based framework to improve power system resilience and reliability. PMAPS (IEEE International Conference on Probabilistic Methods Applied to Power Systems), 2018, 1-6.

Vaiman, M., R. Quint, A. Silverstein, M. Papic, D. Kosterev, N. Leitschuh, A. Faris, S. Yang, B. Blevins and S. Rajagopalan. 2018. Using synchrophasors to improve bulk power system reliability in North America. PESGM (IEEE Power & Energy Society General Meeting), 2018, 1-5.

Wong, L. A., H. Shareef, A. Mohamed and A. A. Ibrahim. 2014. An enhanced opposition-based firefly algorithm for solving complex optimization problems (Algoritma kelip berasaskan teori tentangan untuk penyelesaian masalah pengoptimuman kompleks). *Jurnal Kejuruteraan* 26: 89-96.

Yadav, A. and V. Mahajan. 2021. Analysis of structural reliability of complex coefficients fractional-order system using plane transformation. *Journal of Operation Automation in Power Engineering*.